MINISTRY OF EDUCATION AND TRAINING
HCM CITY UNIVERSITY OF TECHNOLOGY AND EDUCATION

HO NHAT LINH

DEVELOPMENT AND OPTIMIZATION OF GRIPPERS FOR CYLINDER SAMPLES USING COMPLIANT MECHANISMS

Major: Mechanical engineering
Code: 9520103

SUMMARY OF DOCTORAL THESIS

HO CHI MINH CITY – 2023

The work was completed at **Ho Chi Minh City University of Technology and Education**

Supervisor 1: Assoc. Prof. Dr. Le Hieu Giang
Supervisor 2: Dr. Dao Thanh Phong

Reviewer 1:
Reviewer 2:
Reviewer 3:

The thesis will be defended before the Faculty/School level at:
Ho Chi Minh City University of Technology and Education
On month year

LIST OF AUTHOR'S PUBLICATIONS

A. The research results are used in the dissertation

1. **Nhat Linh Ho**, Thanh-Phong Dao, Hieu Giang Le, Ngoc Le Chau (2019). "Optimal Design of a Compliant Microgripper for Assemble System of Cell Phone Vibration Motor Using a Hybrid Approach of ANFIS and Jaya". Arabian Journal for Science and Engineering, 44, 1205–1220. https://doi.org/10.1007/s13369-018-3445-2. (SCIE - Q1).

2. **Nhat Linh Ho**, Thanh-Phong Dao, Ngoc Le Chau, Shyh-Chour Huang (2019). "Multi-objective optimization design of a compliant micro-gripper based on hybrid teaching learning-based optimization algorithm", Microsystem Technologies, 25, 2067–2083. https://doi.org/10.1007/s00542-018-4222-6 (SCIE - Q2).

3. Thanh Phong Dao, **Nhat Linh Ho**, Tan Thang Nguyen, Hieu Giang Le, Pham Toan Thang, Huy Tuan Pham, Hoang Thinh Do, Minh Duc Tran, Trung Thang Nguyen (2017). "Analysis and optimization of a micro displacement sensor for compliant micro-gripper", Microsystem Technologies, 23, 5375–5395. https://doi.org/10.1007 /s00542-017-3378-9 (SCIE - Q2).

4. Ngoc Le Chau, **Nhat Linh Ho**, Ngoc Thoai Tran, Thanh-Phong Dao (2021). "Analytical Model and Computing Optimization of a Compliant Gripper for the Assembly System of Mini Direct-Current Motor". International Journal of Ambient Computing and Intelligence, 12(1), https://doi.org/10.4018/IJACI.2021010101. (SCOPUS)

5. **Nhat Linh Ho**, Minh Phung Dang, Thanh-Phong Dao (2020). "Design and analysis of a displacement sensor-integrated compliant micro-gripper based on parallel structure", Vietnam Journal of Mechanics, 42 (4), 363–374. https://doi.org/10.15625/0866-7136/14874 (ACI)

6. Ngoc Le Chau, **Nhat Linh Ho**, Tran The Vinh Chung, Shyh-Chour Huang, Thanh-Phong Dao (2021). "Computing Optimization of a Parallel Structure-Based Monolithic Gripper for Manipulation Using Weight Method Based Grey Relational Analysis". International Journal of Ambient Computing and Intelligence, 12(3), https://doi.org/10.4018/IJACI.2021070103. (SCOPUS)

7. **Nhat Linh Ho**, Minh Phung Dang, Ngoc Le Chau, Thanh-Phong Dao, Hieu Giang Le (2017). "A hybrid amplifying structure for a compliant micro-gripper", The 10th National Conference on Mechanics, Ha Noi 12/2017, 42. (National Conference).

B. Other published

1. Duc Nam Nguyen, **Nhat Linh Ho**, Thanh-Phong Dao, Ngoc Le Chau (2019). "Multi-objective optimization design for a sand crab-inspired compliant microgripper", Microsystem Technologies, 25, 3991–4009. https://doi.org/10.1007/s00542-019-04331-4 (SCI)

2. **Nhat Linh Ho**, Thanh-Phong Dao, Shyh-Chour Huang, Hieu Giang Le (2016). "Design and Optimization for a Compliant Gripper with Force Regulation Mechanism, International Journal of Mechanical", International Journal of Mechanical, Industrial and Aerospace Sciences, 10.0(12). https://doi.org/10.5281/zenodo.1339720 (International Journal)

3. Ngoc Le Chau, **Nhat Linh Ho**, Minh Phung Dang, Thanh-Phong Dao, Hieu Giang Le (2017). "Optimal Design of a New Compliant Planar Spring for the Upper Limb Movement Support Device with Free Energy Adjustment", The 10th National Conference on Mechanics, Ha Noi 12/2017, 42. (National Conference.

4. **Nhat Linh Ho**, Thanh Phong Dao, Hieu Giang Le (2017). "Analysis of sensitivity of a compliant micro-gripper", Journal of Technical Education Science, 42, 53-61. (UTE – HCMC, Domestic Journal)

Chapter 1 INTRODUCTION

1.1. Background and motivation

Robotic grippers were created to replace or aid humans in repetitive, dirty, or dangerous tasks. They are used in various fields, such as medical, biology, material handling, automated assembly lines, and machine tending. Industrial robotic grippers are preferred for complex assembly tasks, as labor costs rise and gripper costs decrease. There are four basic types of robotic grippers: electric, pneumatic, hydraulic, and vacuum. Traditional grippers have limitations such as bulky requirements, multiple components, and high maintenance costs. Compliant grippers have been developed to address these issues, as they have a monolithic structure, fewer components, lower friction and lubrication requirements, are lightweight, and have lower costs. However, there is a lack of development of displacement sensors for compliant grippers, which can direct-online observe stroke and forces. Additionally, there is no research related to compliant grippers for DC motor assembly systems. Therefore, the motivation for this thesis is to develop an asymmetrical CG with an integrated displacement sensor for self-measurement of the jaw's stroke and a symmetrical CG for handling cylinder shafts in DC motor assembly applications. The study results will contribute to the development of techniques for designing, analyzing, and optimizing compliant grippers for the assembly industry.

1.2. Problem description of proposed compliant grippers

This dissertation proposes two compliant grippers for gripping and releasing cylinder samples for DC motor assembly, with a focus on assembling small electronic components such as the shaft and core of a vibrating motor for mobile phones (Figure 1.3). The first problem addressed is how to measure the displacement of the gripper jaws quickly and precisely, while the second problem is how to enhance the stroke and speed of the gripper. To solve these problems, the dissertation presents an asymmetrical gripper with a displacement sensor and

a symmetrical gripper optimized for improved stroke and resonant frequency.

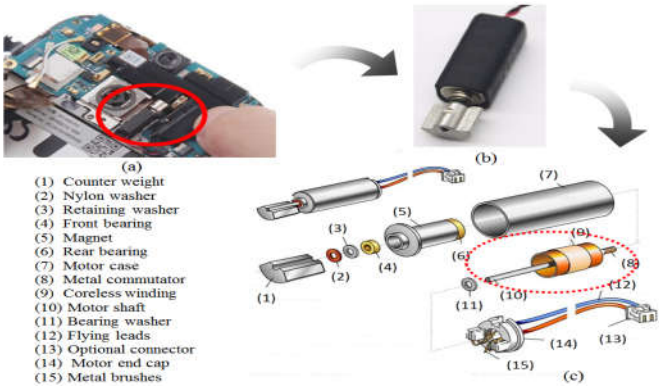

Figure 1.3: A miniatured vibrating motor: a) Mobile phone, b) Vibrating mobile-phone motor, c) Miniatured motor [1]

1.3. Objects of the dissertation

The research objects include as follows: (i) A displacement sensor for the asymmetrical compliant gripper. (ii) A symmetrical compliant gripper for handling cylinder samples.

1.4. Objectives of the dissertation

(i) To develop a displacement sensor for directly measuring the stroke of an asymmetrical compliant gripper; (ii) To develop a symmetrical compliant gripper for handling cylinder samples; (iii) To develop mathematical equations that describe static and dynamic behaviors of the suggested gripers; (iv) To develop new soft-computing-based optimization approaches in improving the performances of proposed compliant gripers.

1.5. Research scopes

According to Ref. [2], the scopes of this dissertation are as follows: (i) Design a new displacement sensor for directly measuring the stroke of the asymmetrical compliant gripper with a range over 1000 μm, a high frequency of over 150 Hz, and a minimal gripping effort; (ii) Design a new symmetrical compliant gripper with a displacement range of over 1000μm and a high frequency of over 60 Hz;

(iii) Formulation of analytical equations to analyze the behaviors of the grippers; (iv) Development of efficient optimization techniques.

1.6. Research methods

The main methods cover in this dissertation are as follows: the finite element method, graphic method, vector method, and analytic method, Pseudo-rigid-body-model approach and Lagrange's principle, statistical techniques, optimization techniques, and experiments.

1.7. The scientific and practical significance of the dissertation

1.7.1. Scientific significance

The scientific significances of the thesis include the following points: (i) Propose a new design principle of displacement sensor; (ii) Develop new design approaches for compliant grippers; (iii) Soft-computing approaches; and (iv) New hybrid optimization approaches.

1.7.2. Practical significance

The practical significances of the thesis include the following points: (i) The developed displacement sensor can self-measure the stroke of the jaws of compliant grippers; (ii) The developed compliant grippers can grip and release cylinder shafts for use in assemble industry as well as food harvester; (iii) The design, analysis, and optimization methods can be employed for compliant grippers as well as related engineering fields; and (iv) The dissertation can be used for referring of post-graduate students.

1.8. Contributions

In terms of sciences: (i) a new design and analysis approach; (ii) new design principles; (iii) soft-computing approaches; and (iv) effective hybrid optimization approaches. ***In terms of applications***: (i) alternative sensors with a low cost; (ii) potential application orientations in assembly lines or food harvester.

1.9. Outline of the dissertation

Chapter 1: Introduction; Chapter 2: Literature review and theoretical foundations; Chapter 3: Design, analysis, and optimization of a displacement sensor for an asymmetrical compliant gripper; Chapter 4: Computational modeling and optimization of a symmetrical compliant gripper for cylindrical samples; Chapter 5: Conclusions and future work

Chapter 2 LITERATURE REVIEW AND THEORETICA FOUNDATIONS

2.1 Overview of compliant mechanism

2.1.1. Definition of compliant mechanism

Similar to traditional rigid mechanisms, flexure hinge-based compliance mechanisms also have the same function as the transfer force, torque, and motion, but are based on the elastic deformation of flexible members (ref.[3]).

2.1.2. Categories of compliant mechanism

2.1.2.1. Compliance-driven classification [4]

2.1.2.2. Deformation-based classification [4]

2.1.2.3. Classification based on the association of the compliance and movement segments of the mechanism [5]

2.1.2.4. Classified based on the function [6]

2.1.3. Compliant joints or flexure hinges

The research findings in references [7] suggest that the leaf hinge with a rectangular cross-section is the best option for the suggested grippers.

2.2 Actuators

Piezoelectric actuators are preferred for operating compliant mechanisms due to their small size, accurate displacement, and fast response.

2.3 Displacement amplification based on the compliant mechanism

This section presents some of the notable research studies on amplification structures such as:

2.3.1. Lever mechanism

2.3.2. The Scott-Russell mechanism

2.3.3. Bridge mechanism

The thesis uses the Leverage structure due to its exceptional benefits, such as a higher amplification ratio, efficiency, simplicity, and low cost.

2.4 Displacement sensors based on compliant mechanisms

To ensure reliable operation, compliant mechanisms need to control position changes, but commercial sensors can be expensive. To address this issue, researchers have developed integrated sensors using techniques like strain gauges [8], [9]. By integrating displacement sensors into compliant grippers, benefits such as working space, control, precision, force feedback, and safety can be achieved, but the implementation depends on the gripper's structure. In this context, the dissertation presents a monolithically integrated displacement sensor designed for an asymmetric gripper.

2.5 Compliant grippers based on embedded displacement sensors

Compliant grippers are of two types: with or without sensors. Grippers without sensors are cheaper but less precise, while those with sensors are more expensive but offer greater control. The choice of gripper depends on the required level of precision for the application [2], [10].

2.6 International and domestic research

2.6.1. Research works in the field by foreign scientists

2.6.1.1. Study on compliant mechanisms by foreign scientists

Compliance mechanisms emerged in the 1960s and gained traction in the 1990s. Several authors in the field have proposed different models and techniques, such

as Howell and Midha (1994) [11], Chen et al. (2023) [12], and so on. See Refs. [13] for more information.

2.6.1.2. Study on robotic gripper and compliant gripper by foreign scientists

Various grippers have been developed by the robotics industry for different applications, including industrial manufacturing, biomedical, product grading, and packaging. Studies by researchers such as Hujic et al. (1998) [14], Lee et al. (2020) [15], Qiu et al. (2023) [16] have been conducted. There have also been studies on compliant grippers by Sun et al. (2013) [17], Hao and Zhu (2019) [18], among others, with a comprehensive overview provided in reference [19]. However, no compliant gripper for picking, positioning, and releasing objects with cylindrical profiles has been demonstrated for application, specifically for a vibrating motor "shaft and core" assembly system.

2.6.2. Research works in the field by domestic scientists

2.6.2.1. Research on compliant mechanisms by Vietnamese scientists

A survey conducted in Vietnam showed that there are currently very few research groups working on compliant mechanism. The groups that have been identified include Pham's, Tran's, Dao's, Dang's, and another Pham's research group. Vietnamese researchers have only recently started to work on this field, beginning in the 2010s. Pham et al. (2013) [20], Dao and Huang (2016) [21]. Tran et al. (2018)[22], Nguyen et al. (2021) [23], and Chau et al. (2021) [24].

2.6.2.2. Research on robotic grippers and compliant grippers by Vietnamese scientists

The development of the robotic gripper industry in Vietnam has been significant in recent years, thanks to research and the application of technology in production and fabrication. Several studies have been conducted by domestic researchers, including Anh et al. (2016)[25], Nguyen and colleagues (2022) [26], etc. Compliant grippers have also been of interest recently, with studies by Lam et al (2017) [27], Nguyen et al (2022) [28], etc. However, no similar research to

the proposed gripper in this dissertation has been conducted.

2.7 Overview of theoretical foundations for compliant mechanisms

2.7.1. Design of experiments

2.7.1.1. Response surface method

In this dissertation, the Response surface method is a statistical technique used for connecting between the input factors and the response variable [29].

2.7.1.2. Taguchi method

This thesis uses Taguchi method's parameter design to plan experiments and find optimal solutions, based on two criteria: (i) Smaller-the-better, and (ii) Larger-the-better.

2.7.2. Modeling methods and approaches for compliant mechanisms

2.7.2.1. Analytical methods

In this thesis, the following methods are used to describe the behavior of gripper

a) Pseudo-rigid-body model

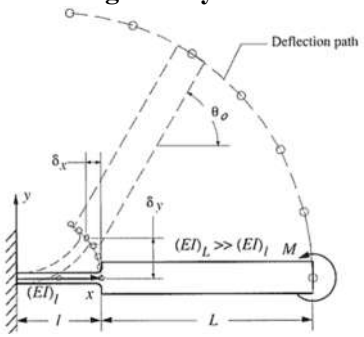

Figure 2.25: A cantilever beam.

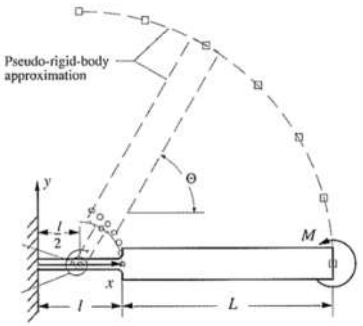

Figure 2.26: PRBM of a cantilever beam.

To analyze the behavior of a compliant gripper under large and nonlinear deflections, this thesis utilizes the Pseudo-rigid-body model (PRBM)[30], which replaces rigid body components with flexible members (i.e., torsional springs) with equivalent force-deflection properties (see Figure 2. 25and Figure 2.26).

b) Lagrange-based dynamic modeling approaches

The dynamic equation is determined by Lagrange's equation:

$$\frac{d}{d_t}\left(\frac{\partial T}{\partial \dot{y}}\right)-\frac{\partial T}{\partial y}+\frac{\partial V}{\partial y}=0, \tag{2. 1}$$

where y denotes input displacement, V represent he potential energy, T is the kinetic energy.

Through the relationship between V, T, K_{ds} and M of the springs, natural frequency (f) is calculated through the following Eq. (2.11) as:

$$f=\frac{1}{2\pi}\sqrt{\frac{K_{ds}}{M}}, \tag{2. 2}$$

c) Finite Element Method

In this dissertation, a nonlinear FEA in ANSYS software was utilized to analyze the object's static and dynamic behavior [31].

d) Graphic method, Vector method, and analytic method

In this thesis, Graphic method, Vector method, and analytic method to describe the motion and behavior properties of gripper. See ref [32] for more details.

2.7.2.2. Data-driven modeling methods

The dissertation utilizes ANFIS [33], a data-driven modeling technique, to establish the relationship between the design variable and output response of the optimization problem.

2.7.3. Statistical methods

In this study, ANOVA [34] was used to examine the sensitivity of design parameters and demonstrate the significant contributions of each design factor to the quality output response.

2.7.4. Optimization methods

2.7.4.1. Metaheuristic algorithms

Metaheuristic algorithms are used to solve difficult problems that exact methods

cannot handle. They use a heuristic approach to refine or explore new solutions over time. Popular algorithms include GA, PSO, SA, Tabu search, TLBO, and Jaya. TLBO and Jaya were used in this dissertation.

2.7.4.2. Data-driven optimization

Data-based optimization involves collecting, analyzing, optimizing, evaluating, and continuously improving data. Methods such as TM, GRA, TLBO, and ANFIS are used for their advantages such as easy implementation and fast convergence. TLBO, ANFIS, and Jaya techniques are utilized in this dissertation.

2.7.5. Weighting factors in multi-objective optimization problems

Weighting factors (WF) are used in multi-objective optimization problems (MOOPs) to balance the importance of different objectives. They can be assigned by the decision maker or determined using formal methods such as direct assignment, eigenvector method, or means of bivariate statistics [35]–[38]. In this thesis, a statistical method is used to calculate the weighting factors.

2.8 Summary

This chapter covers topics related to compliant mechanism and its applications. It discusses the history, classification, and commonly used FHs of compliant mechanisms. It presents the concept of actuators suitable for compliant mechanisms and integrating displacement sensors into grippers. Additionally, it provides an overview of research on compliant mechanisms, robotic and compliant grippers. Finally, it introduces analytical and computational optimization techniques relevant to the thesis.

Chapter 3 DESIGN, ANALYSIS, AND OPTIMIZATION OF A DISPLACEMENT SENSOR FOR AN ASYMMETRICAL COMPLIANT GRIPPER

3.1 Research targets of displacement sensor for compliant gripper

This chapter aims to solve the direct measurement of the jaw's stroke of grippers

by considering two main issues. Firstly, a displacement sensor will be developed and integrated into the gripper, improving its economy and reducing bulkiness. Secondly, a new approach will be proposed for the analysis, design, and optimization of CGs, which includes an exact WF value calculation technique. Technical requirements of the proposed gripper will be presented in section 3.2.2.

3.2 Structural design of proposed displacement sensor

3.2.1. Mechanical design and working principle of a proposed displacement sensor

3.2.1.1. Description of structure of displacement sensor

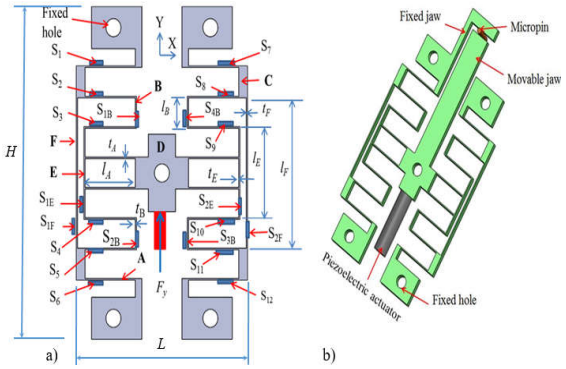

Figure 3.1: Design structure: (a) Displacement sensor and (b) Asymmetrical compliant gripper**.**

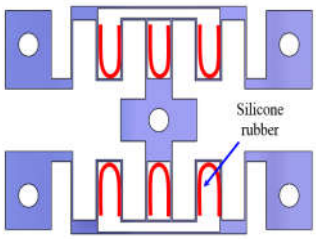

Figure 3.2: Silicon rubber is reinforced along the contour of the cavity.

The suggested displacement sensor consists of a mobile platform, and integrated strain gauges as Figure 3.1(a). The platform is designed to work with an asymmetrical compliant gripper as shown in Figure 3.1(b). The FHs include A, B, E, and F types. The elastic bodies are glued by strain gauges on the FH surfaces (S_1~S_{12}), (S_{1B}~S_B), and (S_{1E}, S_{2E}, S_{1F}, S_{2F}). Fabrication material is Al7075. Silicon rubber (SR) is used to improve the platform's stiffness (Figure 3.2).

3.2.1.2. Design calculation of displacement sensor

To facilitate the design of a displacement sensor, a half-Wheatstone bridge circuit is employed, in Figure 3.3. The diagram of this picture can be found in [39]. The strain sensor's gauge factor can calculate by the following equation:

$$G = \frac{\Delta R}{R \times \varepsilon}, \qquad (3.\ 1)$$

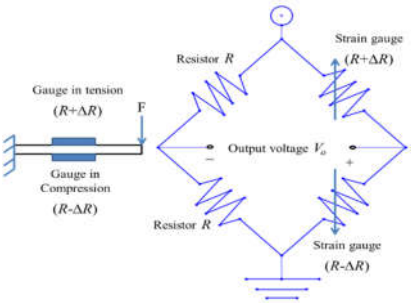

Figure 3.3: A proposed half-Wheatstone bridge circuit

Through the process of mathematical analysis, sensitivity of strain gauge, and S is calculated by equation (3.10):

$$S = \frac{3V_{ex}Gt_A}{l_A^2}, \qquad (3.\ 2)$$

This value can be measured by considering the output displacement of the platform of displacement sensor and the output voltage.

3.2.2. Technical requirements of a proposed displacement sensor

To grip the shaft of a DC motor with a shaft diameter of 600-800 µm[2], the displacement sensor must meet specific specifications, including a large displacement measurement range (>1000 µm), high frequency (>150 Hz), and minimum gripping force.

3.3 Behavior analysis of the displacement sensor

3.3.1. Strain versus stress

In this section, appropriate locations are identified to embed strain gauges into the platform. Strain and stress are connected through Hooke's law. This analysis is performed in two cases: (i) Fabrication of samples for experimentation and (ii) FEM analysis. In addition to increasing the rigidity of the structure, Silicone rubber is also added to the platform in the required positions. Results were obtained at each location in 3 cases: (i) Experiment with SR; (ii) Experiment without SR; and (iii) FEAs without SR were compared. Due to the symmetrical construction of the gripper, only haft of the structure (groups A, B, E, and F of

FHs on the left side positions) are assessed. Experiment is setup as shown in Figure 3.4. The strain of each position was measured separately. The experiments were measured 5 times. Force was increased gradually with values of 2.2 N, 4.6 N, and 7.8 N. The results obtained at the locations where the strain gauges are attached are listed in Table 3.4 and graphed for comparison similar to Figure 3.9. As stated in Table 3. 4, the highest stress was at position (S2B), followed by (S2E) and (11), with group F having the lowest stress. Necessitating its careful consideration due to its impact on the platform's fatigue life.

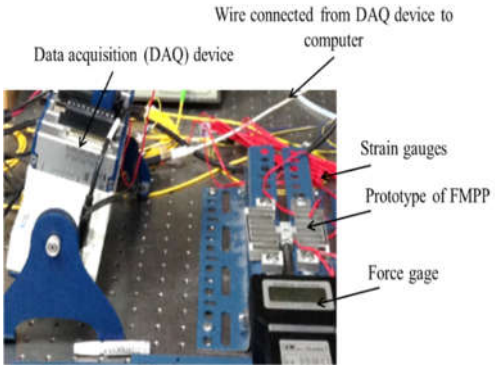

Figure 3.4: Measured strain for displacement sensor platform.

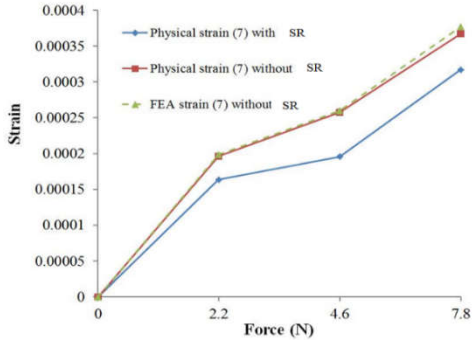

Figure 3.9: Relationship between strain and position (7) for group A in situations where SR is filled and where it is absent.

Table 3.4: Stress values at various positions.

Measuring position	**Corresponding stress (MPa)**
Position (7)	26.78
Position (8)	60.94
Position (9)	51.93
Position (10)	51.62
Position (11)	70.48
Position (12)	41.05
Position (S_{1B})	37.49
Position (S_{2B})	85.31
Position (S_{1E})	32.14
Position (S_{2E})	73.13
Position (S_{1F})	9.91
Position (S_{2F})	25.57

3.3.2. Stiffness analysis

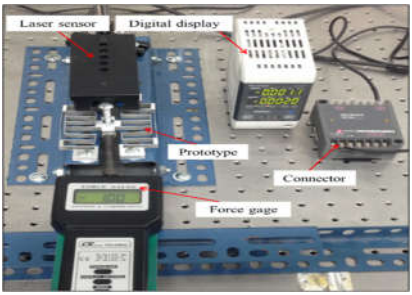

Figure 3.23: Experiment fort measuring the displacement of displacement sensor.

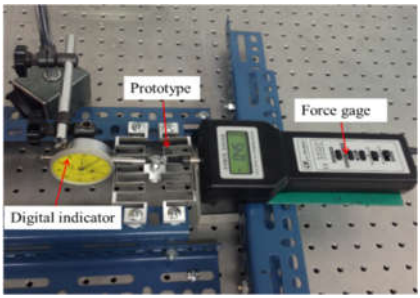

Figure 3.24: Measurement of stiffness in *x*-direction of displacement sensor.

Table 3.5: Displacement with various forces.

Displacement (μm)	**Force (N)**			
	0.25	0.5	0.85	1.3
Experiment: no SR	125	164	288	352
Experiment: with SR	86	91	153	200
FEA: no SR	128	172	294	356
FEA: with SR	94.0	110	158	210

Table 3.6c: Displacement along the *x*-direction.

Displacement (μm)	**Force (N)**			
	0.25	0.5	0.85	1.3
Experiment: no SR	30	50	70.0	140
Experiment: with SR	20	30	40.0	110
FEA: no SR	34	48	64.0	143
FEA: with SR	23	33	45.0	114

The SR not only served to fortify the platform, but also leveraged the body's elasticity to alter its dynamic response. Experiments and simulations were conducted to study this trait, comparing performance with and without the filled SR under different force conditions. The prototype was immobilized and displacement was measured using a laser displacement sensor. The experiment was repeated four times. Experiment is setup as shown in Figure 3.23. Table 3.5 shows that incorporating the viscoelastic SR enhanced the stiffness of the displacement sensor from 0.002 N/μm to 0.003 N/μm, indicating the potential to improve flexure-based micro-positioning platform design by adding more SR. Experimental and simulation results aligned. Numerous experiments and simulations were performed to increase stiffness, focusing on x-axis load. Forces

of 0.25 N, 0.5 N, 0.85 N, and 1.3 N were applied and displacement was measured (Fig. 3.24). Stiffness increased from 0.008 N/µm to 0.012 N/µm with SR-embedded case (Table 3.6), indicating an overall increase in stiffness.

3.3.3. Frequency response

The experiment aimed to test the dynamic characteristics of the platform within a certain frequency range (Figure 3.25 & Figure 3.26). The natural frequency was measured with and without an embedded SR, which increased the stiffness and response speed of the platform. The PEA was also measured with and without the SR, and the results showed an increase in stiffness from 149 Hz to 223 Hz. The data is presented in Table 3.7.

Table 3.7: First natural frequency.

No PEA and no SR (Hz)	**No PEA with embedded SR** (Hz)	**With PEA but no SR** (Hz)	**With PEA with embedded SR** (Hz)
109.8	110.3	149	223

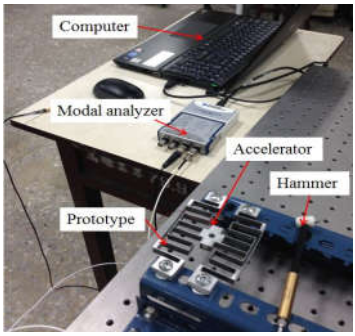

Figure 3.25: Experiments for measuring frequency by hammer.

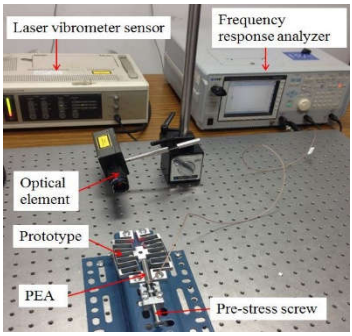

Figure 3.26: Experiments for measuring frequency with exerted PEA.

Embedding the SR within the open cavities increased the frequency, indicating a significant impact on the positioning platform's stiffness. A compliant platform that becomes stiffer will operate more efficiently at higher frequencies, resulting in improved speed and performance.

3.4 Design optimization of a proposed displacement sensor

3.4.1. Description of optimization problem of a proposed displacement sensor

3.4.1.1. Definition of design variables

The optimization problem is briefly presented as follows: $\boldsymbol{X} = [l_A, l_B, t_A, t_B, t_E, t_F]^T$. The minimum and maximum values assigned to the design variables: 15 mm $\leq l_A \leq$ 35 mm; 7 mm$\leq l_B \leq$ 17 mm; 0.5 mm $\leq t_A \leq$ 1.0 mm; 0.5 mm $\leq t_B \leq$ 0.9 mm; 0.5 mm $\leq t_E \leq$ 1.2 mm; 0.5 mm $\leq t_F \leq$ 1.5 mm.

3.4.1.2. Definition of objective functions

Three main cost functions are included. (i) Max $f_1(\boldsymbol{X})$ (the displacement of gripper), (ii) Max $f_2(\boldsymbol{X})$ (a first natural frequency), and (iii) Min $f_3(\boldsymbol{X})$ (the gripping effort).

3.4.1.3. Definition of constraints

The compliant gripper is only efficiency worked in elastic limit of AL-7075. Therefore, it has a constraint involved in safety condition as: $g(x) = \sigma \leq (\sigma_y/S)$. Where σ_y is yield strength of Al-7075 and safety factor S of 1.5 is selected to ensure a safety condition.

3.4.1.4. The proposed method for optimizing the displacement sensor

The process consists of two steps. Firstly, the Taguchi method is used to organize experiments and evaluate the design parameters' influence on output responses. This technique limits the search space and determines the weight value for each design objective accurately. Secondly, the teaching-learning-based optimization algorithm uses the search space and weight value from step 1 to optimize the problem.

3.4.2. Optimal Results and Discussion

3.4.2.1. Determining Weight Factor

To conduct the experiment, the design variable was split into three levels using Taguchi's L_{27} orthogonal array. Grip effort, displacement, and the first natural frequency were analyzed using the *S/N* ratio. ANOVA analysis was used to

determine the impact of design parameters on the output response. Hence, The search space is limited as follows:

Case 1: for displacement

$$\begin{cases} 25\ \text{mm} \le l_A(A) \le 35\ \text{mm} \\ 12\ \text{mm} \le l_B(B) \le 17\ \text{mm} \\ 0.5\ \text{mm} \le t_A(C) \le 0.75\ \text{mm}. \\ 0.5\ \text{mm} \le t_B(D) \le 0.9\ \text{mm} \\ 0.5\ \text{mm} \le t_E(E) \le 0.85\ \text{mm} \end{cases}$$

Case 2: for frequency

$$\begin{cases} 15\ \text{mm} \le l_A(A) \le 25\ \text{mm} \\ 7\ \text{mm} \le l_B(B) \le 12\ \text{mm} \\ 0.75\ \text{mm} \le t_A(C) \le 1.0\ \text{mm}. \\ 0.5\ \text{mm} \le t_B(D) \le 0.7\ \text{mm} \\ 0.85\ \text{mm} \le t_E(E) \le 1.2\ \text{mm} \end{cases}$$

Case 3: for gripping effort

$$\begin{cases} 7\text{mm} \le l_B(B) \le 12\text{mm} \\ 0.5\text{mm} \le t_A(C) \le 0.75\text{mm}. \\ 0.7\ \text{mm} \le t_B(D) \le 0.9\text{mm} \end{cases}$$

Then, the WF for each response is determined as follows (Table 3.18, 3.19, 3. 20):

Table 3.18: The WF for the displacement.

Level	**The average of the normalized S/N ratios for each level**					
	A	B	C	D	E	F
Level 1	0.2102	0.4645	0.7054	0.5653	0.5668	0.5293
Level 2	0.5587	0.5440	0.4939	0.4994	0.5113	0.5231
Level 3	0.7957	0.5560	0.3653	0.4998	0.4864	0.5121
Range r_{ij}	0.5855	0.0915	0.3401	0.0660	0.0804	0.0172
w_1 = **0.3083**						

Table 3.19: The WF for the frequency.

Level	**The average of the normalized S/N ratios for each level**					
	A	B	C	D	E	F
Level 1	0.8700	0.7625	0.3857	0.5797	0.4969	0.5409
Level 2	0.5480	0.5302	0.6090	0.5509	0.5666	0.5410
Level 3	0.2350	0.3603	0.6583	0.5224	0.5895	0.5711
Range r_{ij}	0.6350	0.4022	0.2725	0.0573	0.0926	0.0302
w_2 = **0.3891**						

Table 3.20: The WF for the gripping effort.

Level	**The average of the normalized S/N ratios for each level**					
	A	B	C	D	E	F
Level 1	0.6766	0.6227	0.4661	0.6982	0.5403	0.6515
Level 2	0.6137	0.4357	0.6343	0.6326	0.5974	0.5464
Level 3	0.5007	0.7326	0.6906	0.4602	0.6533	0.5931
Range r_{ij}	0.1760	0.2968	0.2245	0.2380	0.1130	0.1051
w_3 = **0.3026**						

3.4.2.2. Optimal results

After the weight factors are determined, the optimization is performed for all 3 cases (#case 1, #case 2, and #case 3). The results show that, the function fval of case 3 is the best (# case 1: f_{val} = -1.4288; # case 2: f_{val} = -1.6129; # case 3: f_{val} = -1.6190). Therefore, case 3 was the most suitable solution for the gripper design. The optimal design parameters for case 3 are: X_{val} = [15; 11.67; 0.62; 0.86; 0.7; 1.25] ~ $[l_A, l_B, t_A, t_B, t_E, t_F]^T$. In addition, the optimal results obtained from the proposed algorithm are also compared with the results obtained from other methods such as PSO, AEDE and GA.

3.4.3. Verifications

A compliant gripper was designed using Case 3 and tested with ANSYS 16 software. A prototype was manufactured and tested using a force gauge and laser displacement sensor. The gripper's first natural frequency was also tested with a PEA and high nanoscale resolution laser vibrometer sensor (refer to Figure 3.31).

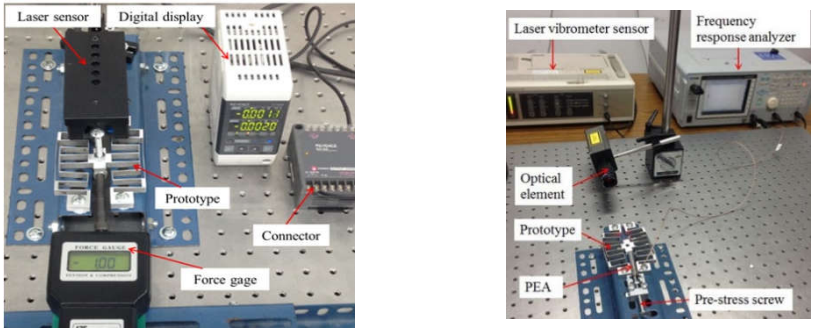

(a) (b)

Figure 3.31: Experimental tests: (a) Displacement and (b) Frequency.

In the strain test shown in Figure 3.32, a 5 N force was applied from a force gauge, and sensor gauges attached to the FHs measured the actual strain, with measurements taken five times.

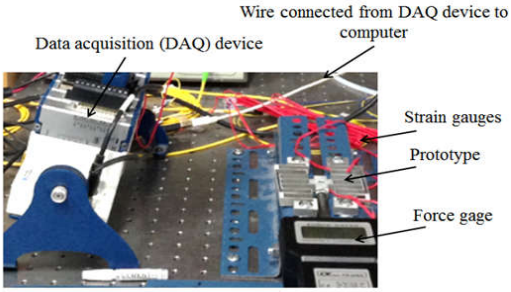

Figure 3.32: Test of physical strain.

Table 3. 27 shows that the experimental results are close to the predicted results.

Table 3.27: Experimental results.

Quality outcome	HTLBO	Experiment	FEA	Error (%) between HTLBO and experiment	Error (%) Between HTLBO and FEA
Displacement (μm)	1924.15	1831.40	1845.15	4.82	4.10
Frequency (Hz)	170.45	164.63	164.90	3.41	3.25
Stress (MPa)	46.71	44.54	44.06	4.64	5.67

3.5 Summary

In this chapter, the results show that (i) the developed CG met the initial hypothesis with a displacement of 1924.15 μm, a frequency of 170.45 Hz, and a maximum stress of 46.71 MPa; (ii) the proposed algorithm outperformed other optimizers; (iii) the HTLBO produced better optimal solutions than other algorithms; and (iv) the predicted results matched well with both simulation and empirical validations.

Chapter 4 COMPUTATIONAL MODELING AND OPTIMIZATION OF A SYMMETRICAL COMPLIANT GRIPPER FOR CYLINDERICAL SAMPLES

4.1 Basic application of symmetrical compliant gripper for cylinder samples

A symmetrical compliant gripper (Figure 4.1) has been developed to meet the practical requirement for assembling a DC vibrating motor system (Figure 1.3, Chapter 1). The gripper is used to manipulate the shaft towards the core of a mobile phone vibration motor. The shaft size ranges from 600-800 μm [40].

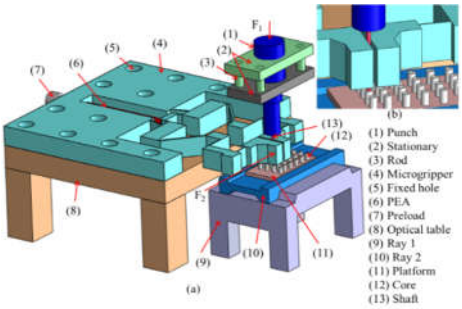

Figure 4.1: Assemble system for the mini vibrating motors: (a) Assembling system, (b) Details of motor shaft and core.

4.2 Research targets of symmetrical compliant gripper

Two targets were identified for designing a gripper for the DC motor assembly: (i) developing a compliant gripper for locating and gripping shaft-type parts of a vibrating motor used in mobile phones, with technical requirements presented in section 4.3.2; and (ii) creating an optimized compliant gripper with a focus on ease of use, reliability, and economic efficiency.

4.3 Mechanical design of symmetrical compliant gripper

4.3.1. Description of structural design

Ho et al. [41] developed a gripper suitable for vibrating DC motor assembly [20]. It uses a simple, stiff, square wave signal type with an elastic FHs for motion (Figure 4.2 (a-c)), a displacement amplification mechanism (Figure 4.3), and a piezoelectric actuator for force generation. The left hand matches the right hand's displacement and gripping, with preload ensuring good initial interference. Sine or cosine wave signals would increase the gripper's topology complexity.

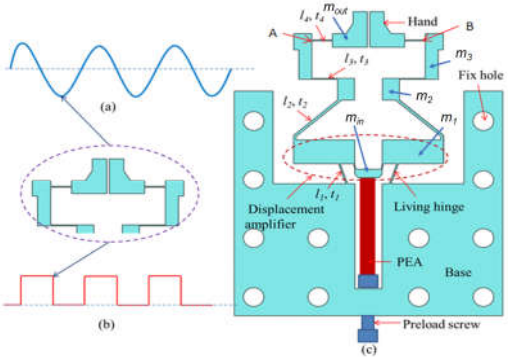

Figure 4.2: CAD model: (a) Sine shape, (b) Rectangular shape and (b) Symmetric compliant gripper.

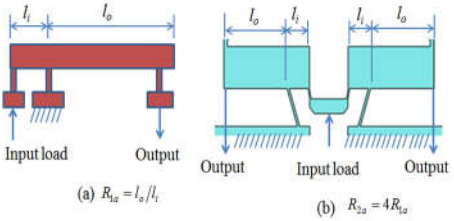

Figure 4.3: Levers: (a) Lever mechanism, (b) Double lever mechanism.

4.3.2. Technical requirements of proposed symmetrical compliant gripper

The proposed symmetrical CG must meet the following specifications: (ii) Hand grips are constructed with a square wave design. This model can ensure that both

jaws move symmetrically; (ii) Having a large displacement measurement range (>1000μm), and a high frequency (> 60Hz); (iii) The equivalent stress of CG must be lower than yield stress of the material; and (iv) The gripper may have a DA ratio of up to 12.

4.3.3. Behavior analysis of the proposed compliant gripper

In this section, through the geometry relation of the stiffener, and joint. The gripper behavior is analyzed. In addition, the analysis process also allows for predicting the movement trend of the gripper. then, the design parameters are adjusted to fit the design target.

4.3.3.1. Kinematic analysis

4.3.3.2. Stiffness analysis

4.3.3.3. Static analysis

4.3.3.4. Dynamic analysis

4.4 Design optimization of the compliant gripper

4.4.1. Problem statement of optimization design

To meet the design goal, the gripper must meet the following requirements: (i) Having a high first natural frequency for a large operating bandwidth and prevents resonance with the excitation frequency of actuators; (ii) Having a large working; (iii) Having a small resulting stress to achieve good strength criteria of the gripper.

4.4.1.1. Determination of design variables

The optimization problem is briefly presented as follows: $\boldsymbol{X} = [l_0, l_i, l_1, l_2, l_3, l_4, t_1, t_2, t_3, t_4]^T$. The minimum and maximum values assigned to the design variables: 10 mm $\leq l_1 \leq$ 14 mm; 20 mm$\leq l_2 \leq$ 24 mm; 11 mm $\leq l_3 \leq$ 15 mm; 6 mm$\leq l_4 \leq$ 10 mm; 0.5 mm $\leq t_1 \leq$ 0.7 mm; 0.8 mm$\leq t_2 \leq$ 1.2 mm; 0.4 mm $\leq t_3 \leq$ 0.8 mm; 0.5 mm$\leq t_4 \leq$ 0.9 mm.

4.4.1.2. Determination of objective functions

Three main cost functions are included. (i) Max $f_1(\boldsymbol{X})$ (the displacement of

gripper), (ii) Max $f_2(\boldsymbol{X})$ (a first natural frequency).

4.4.1.3. Determination of constraints

The CG is only efficiency worked in elastic limit of AL-7075. So, it has a constraint involved in safety condition as: $g(x) = \sigma \leq (\sigma_y/S)$. where σ_y is yield strength of Al-7075 and safety factor S of 1.5.

4.4.2. Proposed optimization method for the compliant gripper

In this section, integration of an ANFIS with the Jaya was used to implement the optimization problem. MATLAB R2015b was used to perform the programming. Figure 4. 8 illustrates a flowchart for optimizing process.

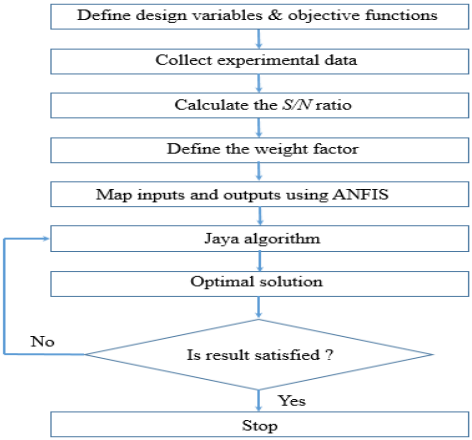

Figure 4.8: Flowchart of multi-objective optimization.

4.4.3. Optimized results and validations

4.4.3.1. Optimized results

After the experiment is organized by Taguchi's L_{27} orthogonal array. Data is collected. The *S/N* ratio is calculated. The WF of each response is calculated correctly (Table 4.5 & 4.6).

Table 4.5: WF of displacement response

Level	**The average of the normalized S/N ratios for each level**							
	A	B	C	D	E	F	G	H
Level 1	0.6137	0.3447	0.3257	0.3437	0.4109	0.2978	0.3579	0.3371
Level 2	0.2426	0.2761	0.2769	0.3009	0.3426	0.4588	0.3163	0.3158
Level 3	0.1368	0.3723	0.3905	0.3485	0.2396	0.2365	0.3189	0.3762
Range r_{ij}	0.4769	0.0963	0.1136	0.0476	0.1713	0.2223	0.0417	0.0604
w_1 = 0.5202								

Table 4.6: WF of frequency response

Level	The average of the normalized S/N ratios for each level.							
	A	**B**	**C**	**D**	**E**	**F**	**G**	**H**
Level 1	0.6490	0.7846	0.7246	0.6515	0.5899	0.6865	0.5884	0.6539
Level 2	0.7230	0.7265	0.6563	0.7557	0.7588	0.6394	0.6504	0.7716
Level 3	0.7168	0.5777	0.7080	0.6816	0.7402	0.7630	0.8500	0.6447
Range r_{ij}	0.0739	0.2069	0.0683	0.1041	0.1689	0.1236	0.2616	0.1270
w_2 = **0.4798**								

ANFIS is used to build relationships between design variables and output responses through a black box. Jaya is applied to perform the optimization process. The optimized solutions were determined are l_1 = 10.0 mm, l_2 = 20.6 mm, l_3 = 11.2 mm, l_4 = 6.0 mm, t_1 = 0.5 mm, t_2 = 0.8 mm, t_3 = 0.4 mm, t_4 = 0.9 mm. The ideal displacement and frequency were found to be approximately 3260 µm and 61.9 Hz, respectively. The performance of the JA-ANFIS optimization algorithm was compared with other emerging methods. Although the optimal solutions were similar, the JA-ANFIS algorithm demonstrated a faster convergence rate and consumed significantly less time (Table 4.8).

Table 4.8: Comparison of several optimization techniques.

Approach	Analysis time (sec)	Generation	Displacement (µm)	Frequency (Hz)
NGSA-II ANFIS	787.3	1000	3260	61.9
TLBO-ANFIS	660	500	3260	61.9
Jaya-ANFIS	30.0	44	3260	61.9

4.4.3.2. Validations

After optimization, the prototype with the design parameter is the optimal value and the thickness of 10 mm is fabricated for experimental verification. Experiment is set up as shown in Figure 4.9.

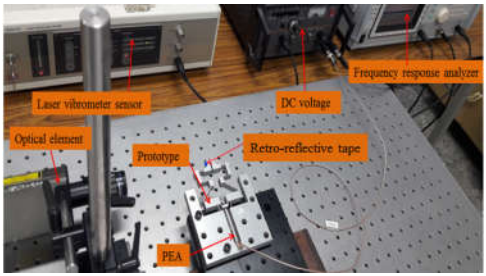

Figure 4.9: Experiment setup for the prototype.

The experiments were performed five times, and the average values were recorded in Table 4. 9. In addition, FEA was also performed and the results compared.

Table 4.9: The optimum, FEA, and experimental outcomes are compared.

Performances	Optimal results	FEA	Experiment	Errors between optimized and FEA results (%)	Errors between optimized and experimental results (%)
Displacement(μm)	3260	3097	3064	5.26	6.39
Frequency (Hz)	61.9	59.42	58.18	4.16	6.38

4.5 Conclusions

This section outlines the best design of the CG for assembling cell phone vibration motors. The CG is intended to handle the shaft towards the core of the motor and has a displacement amplification 11 times greater than the input displacement. Multi-objective optimization was used to design the CG, with the displacement and resonant frequency chosen as objective functions. The optimal analysis was conducted using the Taguchi method, S/N ratios, ANFIS, and Jaya algorithm. The best parameter values and optimal displacement and frequency were determined. The proposed hybrid optimization algorithm was effective and robust, with errors observed ranging from 4.16% to 6.39%.

4.6 Summary

This chapter presents the development of a new symmetrical CG for use in a cylindrical shaft of the DC motor assembly process. A soft computing-based approach was used to model and optimize the proposed gripper, which included the creation of an L-type stroke enlargement mechanism for large working travel. The gripper's form was modeled using the square wave to provide a simple construction and high rigidity. The analytical results were validated through simulations and experiments. An intelligent computational technique was proposed to improve the optimization strategy, which was a combination of ANFIS with JA. The results showed that the developed CG had a displacement

of approximately 3260 μm and a frequency of 61.9 Hz. The proposed hybrid optimization algorithm was also found to be robust and effective compared to other methods. The error between the proposed optimization method and experimental/FEA analysis results was less than 7% for frequencies and displacement, respectively.

Chapter 5 CONCLUSIONS AND FUTURE WORKS

5.1 Conclusions

This dissertation presents the development of two types of compliant grippers for gripping small cylinders used in mobile phone vibration motors. The first gripper has an asymmetrical structure and integrates displacement sensors, while the second has a symmetrical structure and is designed for assembly. The first part of the study analyzes and optimizes the first compliant gripper using strain gauges, SR, and HTLBO, resulting in a displacement of 1924.15 μm and a frequency of 170.45 Hz. In the second part of the study, a CG with two symmetrical jaws for the assembly industry is designed using the pseudo-rigid-body model, Lagrange method, and ANFIS combined with the Jaya algorithm, resulting in an optimal displacement of about 3260 μm and a frequency of 61.9 Hz. Finally, experiments are conducted, and the results show that both compliant grippers are effective, consistent with the theoretical results.

5.2 Future works

In the future, several steps will be taken regarding the proposed displacement sensor and gripper development. First, a prototype of the displacement sensor will be manufactured and tested for sensitivity and resolution. Then, the sensor will be integrated into the asymmetrical gripper to test its self-measured stroke. Next, both asymmetrical and symmetrical grippers will be manufactured and tested on a robot arm for assembling a DC motor in a cell phone to verify their efficiency. Finally, an additional controller will be implemented to examine the precision position and grasping of the gripper jaws.

References

[1] "https://www.precisionmicrodrives.com/eccentric-rotating-mass-vibration-motors-erms," 2022.

[2] N. Le Chau, N. L. Ho, N. T. Tran, and T. P. Dao, "Analytical model and computing optimization of a compliant gripper for the assembly system of mini direct-current motor," *Int. J. Ambient Comput. Intell.*, vol. 12, no. 1, pp. 1–28, 2021, doi: 10.4018/IJACI.2021010101.

[3] R. H. Burns, "The Kinetostatic Synthesis of Flexible Link Mechanisms," Yale University, 1964.

[4] L. Zentner and V. Böhm, "On the classification of compliant mechanisms," *Proceedings of EUCOMES 2008 - The 2nd European Conference on Mechanism Science*. pp. 431–438, 2009. doi: 10.1007/978-1-4020-8915-2_52.

[5] S. G. B. Pratheek Bagivalu Prasanna, Ashok Midha, "Classification of Compliant Mechanisms and Determination of the Degrees of Freedom Using the Concepts of Compliance Number and Pseudo-Rigid-Body Model," 2019.

[6] and Z. H. Heng Wu, Xianmin Zhang, Jinqiang Gan, Hai Li, "High-precision displacement measurement method for three degrees of freedom-compliant mechanisms based on computer micro-vision," *Appl. Opt.*, vol. 55, no. 10, pp. 2594–2600, 2016.

[7] S. Linß, S. Henning, and L. Zentner, "Modeling and Design of Flexure Hinge-Based Compliant Mechanisms," *Kinemat. - Anal. Appl.*, 2019, doi: 10.5772/intechopen.85224.

[8] T.-P. Dao and S.-C. Huang, "Design and analysis of a compliant micro-positioning platform with embedded strain gauges and viscoelastic damper," *Microsyst. Technol.*, vol. 23, no. 2, pp. 441–456, 2016, doi: 10.1007/s00542-016-3048-3.

[9] Z. Chen, Z. Li, X. Jiang, and X. Zhang, "Strain-based multimode integrating sensing for a bridge-type compliant amplifier," *Measurement Science and Technology*, vol. 30, no. 10. 2019. doi: 10.1088/1361-6501/ab1984.

[10] A. N. Reddy, N. Maheshwari, D. K. Sahu, and G. K. Ananthasuresh, "Miniature compliant grippers with vision-based force sensing," *IEEE Trans. Robot.*, vol. 26, no. 5, pp. 867–877, 2010, doi: 10.1109/TRO.2010.2056210.

[11] A. M. L. L. Howell, "A Method for the Design of Compliant Mechanisms With Small-Length Flexural Pivots," *J. Mech. Des.*, vol. 116, no. 1, pp. 280–290, 1994.

[12] J. Chen, R., Wang, W., Wu, K., Zheng, G., Xu, X., Wang, H., & Luo, "Design and optimization of a novel compliant planar parallelogram mechanism utilizing initially curved beams," *Mech. Mach. Theory*, vol. 179, 2023.

[13] B. Zhu *et al.*, "Design of compliant mechanisms using continuum topology optimization: A review," *Mech. Mach. Theory*, vol. 143, p. 103622, 2020, doi: 10.1016/j.mechmachtheory.2019.103622.

[14] D. Hujic, E. A. Croft, G. Zak, R. G. Fenton, J. K. Mills, and B. Benhabib, "The robotic interception of moving objects in industrial settings: Strategy development and experiment," *IEEE/ASME Trans. Mechatronics*, vol. 3, no. 3, pp. 225–239, 1998, doi: 10.1109/3516.712119.

[15] K. Lee, Y. Wang, and C. Zheng, "TWISTER Hand: Underactuated Robotic Gripper Inspired by Origami Twisted Tower," *IEEE Transactions on Robotics*, vol. 36, no. 2. pp. 488–500, 2020. doi: 10.1109/TRO.2019.2956870.

[16] A. Qiu, C. Young, A. Gunderman, M. Azizkhani, Y. Chen, and A.-P. Hu, "Tendon-Driven Soft Robotic Gripper with Integrated Ripeness Sensing for Blackberry Harvesting," *arXiv Prepr.*, vol. 2302.03099, 2023.

[17] X. Sun *et al.*, "A novel flexure-based microgripper with double amplification mechanisms for micro / nano manipulation," vol. 085002, pp. 1–10, 2013.

[18] G. Hao and J. Zhu, "Design of a Monolithic Double-Slider Based Compliant Gripper with Large Displacement and Anti-Buckling Ability," *Micromachines*, vol. 10, no. 10, 2019.

[19] Z. Lyu and Q. Xu, "Recent design and development of piezoelectric-actuated compliant microgrippers: A review," *Sensors Actuators A Phys.*, vol. 331, p. 113002, 2021, doi: 10.1016/j.sna.2021.113002.

[20] D. Wang, J.-H. Chen, and H.-T. Pham, "A constant-force bistable micromechanism," *Sensors Actuators A Phys.*, pp. 481–487, 2013, doi: https://doi.org/10.1016/j.sna.2012.10.042.

[21] D. Thanh-phong and S. Huang, "Multi-objective Optimal Design of a 2-DOF Flexure-Based Mechanism Using Hybrid Approach of Grey-Taguchi Coupled Response Surface Methodology and Entropy

Measurement," 2016, doi: 10.1007/s13369-016-2242-z.

[22] H. Van Tran, T. H. Ngo, N. D. K. Tran, T. N. Dang, T.-P. Dao, and D.-A. Wang, "A threshold accelerometer based on a tristable mechanism," *Mechatronics*, vol. 53, pp. 39–55, 2018.

[23] N. VL, N. VK, and P. HH, "Dynamics Study of Compliant Mechanism with Damping," *J. Appl. Mech. Eng.*, vol. 9, no. 4, 2020.

[24] N. Le Chau, N. T. Tran, and T.-P. Dao, "A hybrid computational method for optimization design of bistable compliant mechanism," *Eng. Comput.*, vol. 38, no. 4, 2020.

[25] N. D. Anh, L. T. Nhat, and T. V. P. Nhan, "Design and Control Automatic Chess-Playing Robot Arm," *Recent Adv. Electr. Eng. Relat. Sci. Lect. Notes Electr. Eng.*, vol. 371, 2016, doi: https://doi.org/10.1007/978-3-319-27247-4_41.

[26] Pho Van NGUYEN, P. N. NGUYEN, T. NGUYEN, and T. L. LE, "Hybrid robot hand for stably manipulating one group objects," *Arch. Mech. Eng.*, vol. 6, no. 3, pp. 375–391, 2022.

[27] D. B. Lam, N. T. Khoa, N. D. Thuan, and P. H. Phuc, "Modeling and force analysis of an electrothermal micro gripper with amplification compliant mechanism," *J. Sci. Technol.*, vol. 119, pp. 22–27, 2017, https://jst.hust.edu.vn/journals/jst.119.khcn.2017.27.4.5

[28] T. T. N. & T.-P. D. Duc Nam Nguyen, Minh Phung Dang, "Intelligent computation modeling and analysis of a gripper for advanced manufacturing application," *Int. J. Interact. Des. Manuf.*, 2022, doi: https://doi.org/10.1007/s12008-022-00885-2.

[29] Mark J. Anderson and P. J. Whitcomb, *RSM simplified: Optimizing Processes Using Response Surface Methods for Design of Experiments*, vol. 53, no. 9. New York: CRC Press, 2019. doi: 10.1017/CBO9781107415324.004.

[30] O. S. Martin Philip Bendsoe, *Topology Optimization: Theory, Methods And Applic*. Springer; 2nd edition (October 4, 2013), 2003.

[31] O. Kessler, "INTRODUCTION TO THE FINITE ELEMENT METHOD," *Rev. Int. Stud.*, vol. 38, no. 1, pp. 187–189, 2012, doi: 10.1017/S0260210511000623.

[32] J. J. Dicker, G. R. Pennock, and J. E. Shigley, *THEORY OF MACHINES AND MECHANISMS*, Third. New York: OXFORD UNIVERSITY PRESS, 2003.

[33] T. V. T. Nguyen, N. T. Huynh, N. C. Vu, V. N. D. Kieu, and S. C. Huang, "Optimizing compliant gripper mechanism design by employing an effective bi-algorithm: fuzzy logic and ANFIS," *Microsyst. Technol.*, vol. 27, no. 9, pp. 3389–3412, 2021, doi: 10.1007/s00542-020-05132-w.

[34] R. W. Emerson, "ANOVA and t-tests," *J. Vis. Impair. Blind.*, vol. 111, no. 2, pp. 193–196, 2017, doi: 10.1177/0145482x1711100214.

[35] H. An, S. Chen, and H. Huang, "Multi-objective optimization of a composite stiffened panel for hybrid design of stiffener layout and laminate stacking sequence," *Struct. Multidiscip. Optim.*, vol. 57, no. 4, pp. 1411–1426, 2018, doi: 10.1007/s00158-018-1918-2.

[36] Z. Li and X. Zhang, "Multiobjective topology optimization of compliant microgripper with geometrically nonlinearity," *Proc. Int. Conf. Integr. Commer. Micro Nanosyst. 2007*, vol. A, pp. 1–7, 2007, doi: 10.1115/MNC2007-21294.

[37] Q. Lu, Z. Cui, and X. Chen, "Fuzzy multi-objective optimization for movement performance of deep-notch elliptical flexure hinges," vol. 065005, pp. 1–9, 2015.

[38] M. Meinhardt, M. Fink, and H. Tünschel, "Landslide susceptibility analysis in central Vietnam based on an incomplete landslide inventory: Comparison of a new method to calculate weighting factors by means of bivariate statistics," *Geomorphology*, vol. 234, no. 2015, pp. 80–97, 2015, doi: 10.1016/j.geomorph.2014.12.042.

[39] N. L. Ho, M. P. Dang, and T.-P. Dao, "Design and analysis of a displacement sensor-integrated compliant microgripper based on parallel structure," *Vietnam J. Mech. Vietnam Acad. Sci. Technol.*, pp. 1–12, 2020, [Online]. Available: http://dx.doi.org/10.1016/j.aquaculture.2013.03.019

[40] N. Le Chau, N. L. Ho, T. T. Vinh Chung, S. C. Huang, and T. P. Dao, "Computing optimization of a parallel structure-based monolithic gripper for manipulation using weight method-based grey relational analysis," *Int. J. Ambient Comput. Intell.*, vol. 12, no. 3, pp. 39–74, 2021, doi: 10.4018/IJACI.2021070103.

[41] N. L. Ho, T. Dao, H. G. Le, and N. Le Chau, "Optimal Design of a Compliant Microgripper for Assemble System of Cell Phone Vibration Motor Using a Hybrid Approach of ANFIS and Jaya," *Arab. J. Sci. Eng.*, vol. 44, no. 2, pp. 1205–1220, 2019, doi: https://doi.org/10.1007/s13369-018-3445-2.